





Nanoparticles of FeNbO₄ Produced by Microwave Assisted Combustion Reaction: a Potential Technology for the Treatment of Wastewater

F. V. de Andrade^{a,*} , C. F. Costa^b, M. R. de Freitas^a , A. C. T. Cabral^a , N. M. Barros^a,
G. M. de Lima^c 

^aUniversidade Federal de Itajubá, Instituto de Engenharias Integradas, Rua Irmã Ivone Drumond, Distrito Industrial II, 35903-087, Itabira, MG, Brasil

^bUniversidade Federal de Itajubá, Instituto de Ciências Puras e Aplicadas, Rua Irmã Ivone Drumond, Distrito Industrial II, 35903-087, Itabira, MG, Brasil

^cUniversidade Federal de Minas Gerais, Departamento de Química, Av. Antônio Carlos, Pampulha, 31270-901 Belo Horizonte, MG, Brasil

Received: April 22, 2020; Revised: July 01, 2020; Accepted: August 10, 2020

Iron(III) niobate, FeNbO₄, was synthesized for the first time by microwave-assisted combustion reaction between Fe(NO₃)₃·9H₂O and NH₄[NbO(C₂O₄)₂(H₂O)₂](H₂O) in the presence of NH₄NO₃ and Urea {O=C(NH₂)₂}. Experiments of X-ray powder diffraction revealed a small crystallite size for this material, 16 nm, and the results of MEV showed that it forms agglomerates with diameters between 80 and 180 nm with spherical shapes. HRTEM images revealed that the material is formed by clusters of particles with a diameter near 20 nm. A surface area of 40 m²g⁻¹ was determined by experiments of specific surface area (SSA). The FeNbO₄ induced the decomposition of H₂O₂, forming radicals that, in turn, discoloured Indigo dye Carmine (IC) a solution. The results showed that this niobate was able to degrade 55% of the initial solution in the presence of H₂O₂ after 360 minutes of reaction time.

Keywords: iron(III) niobate, synthesis by microwave-assisted combustion, advanced oxidative processes, environmental remediation, organic contaminants.

1. Introduction

In the last decades the incorrect disposal of pharmaceuticals, dyes, hazard substances or the misuse of pesticides, among others, have transformed these chemicals in a major environmental problem due to their growing presence in groundwaters. These organic water contaminants normally display slow kinetics of decomposition or biodegradation owing to their chemical and structural stability^{1,2}. Midst the most popular textile colouring agent, stands indigo carmine (IC) or acid blue 74, a well-known anionic dye whose annual production is about millions of tons. Most dyes are carcinogenic and mutagenic, therefore, displays potential toxicity, demanding correct disposal of the industrial wastewaters³⁻⁷. The scientific literature mentions different methodologies studied to remove dyes from wastewater. The so-called advanced oxidative processes (AOP) appears as one of the most promising approaches, especially the catalytic wet hydrogen peroxide oxidation^{8,9}, where H₂O₂ is used as the oxidant for organic contaminants. In recent years, we have developed different catalytic systems to remove organic contaminants in aqueous media⁴⁻⁷.

Recently, there has been an increasing interest in some types of ABO₄ oxides as catalysts, including iron niobate, FeNbO₄. This compound has also been investigated for the applications

as a photodetector, in solar energy conversion, as gas sensor, as photocatalyst and as electrode material for Li-ion batteries¹⁰⁻¹⁴. These compound have three crystalline forms: a wolframite-type (space group p2/c) with a monoclinic symmetry which exists below 1085°C. In a range of 1085 and 1380°C persists the α-PbO₂-type (space group Pbcn) with an orthorhombic symmetry, finally above 1380°C a rutile-type (space group P4₂/mmm) with a tetragonal symmetry is formed. It is also reported a fourth phase that crystallizes in the AlNbO₄-type structure (space group C2/m) with a monoclinic symmetry, stable at 700°C. The degree of the cation order depends on the specific conditions of synthesis^{10,11,13,15,16}. The preparation of the FeNbO₄ powders in most reported works involves solid-state reactions, which generally required long periods of mechanical mixing and high heat treatment temperature to obtain the desired phase, however with low surface area¹³. Among the various approaches, chemical-based methods provide a convenient and simple technique for the synthesis of nanoscale materials. Devesa *et al.* prepared FeNbO₄ powders using the sol-gel method, being observed the formation of the monoclinic phase in the sintered pellets. Fe₂O₃ was detected as an impurity in the range of temperature of 100-500°C, while at 1200°C, single-phase sample was obtained¹¹. Nanospheres of an orthorhombic structure were synthesized by Shim *et al.*¹² using a hydrothermal process at 250°C, obtained with uniform size, in the range of 5-10 nm and a large specific surface area (82.72 m²g⁻¹).

*e-mail: fvqandrade@yahoo.com.br

Cho et al.¹³ synthesized orthorhombic FeNbO₄ nanoparticles by a hydrothermal process followed by calcination at 600°C with an average size of 10-20 nm. In the present study, we report the synthesis and characterization of FeNbO₄ (Fe-Nb) nanoparticles, using for the first time, synthesis by combustion reaction assisted by microwave, to prepare this material. The combustion method is self-sustaining because the high temperatures reached after the beginning of the reaction ensure a rapid formation and crystallization of the powder and the release of a large quantity of gas, which in turn tends to minimize particle agglomeration. This process offers advantages over others, because, it has no subsequent heat treatment steps, obtaining the material directly after the combustion reaction. Another advantage is that the fast microwave preparation of the products consumes less quantity of energy¹⁷⁻²⁰.

A relevant aspect of the present work is the original one-pot synthetic method for the preparation of FeNbO₄. Also, the performance of the material in the catalytic decomposition of aqueous solutions of IC in the presence of H₂O₂ was investigated. It is the first time that FeNbO₄ is used in the literature as a catalyst in the presence of H₂O₂ to remove organic contaminants in an aqueous medium. The results show that the material (Fe-Nb) acts as an activator of H₂O₂, providing an efficient and suitable medium for the degradation of IC in solution.

2. Experimental

2.1 Materials and reagents

NH₄NO₃ (purity ≥ 98%), Fe(NO₃)₃·9H₂O (purity ≥ 98%), and O=C(NH₂)₂ (purity ≥ 99%) were purchased from Sigma-Aldrich and used without further purification. NH₄[NbO(C₂O₄)₂](H₂O)₂ was kindly donated by the CBMM company and used without further purification. Ultrapure water (Millipore Corporation) was used to prepare all aqueous solutions.

2.2 Synthesis

The chemistry of propellants and explosives was explored in the synthesis, where the iron(III) niobate was obtained from the reaction of oxidants and reducing reagents, the latter used as fuel²¹. Urea and NH₄NO₃ were employed as reducing and oxidant agents, respectively, while NH₄[NbO(C₂O₄)₂](H₂O)₂ and [Fe(NO₃)₃·9H₂O] were employed as cation source. The nitrate present in the iron salt has also acted as an oxidant. The stoichiometry for the combustion reaction with more than two components was calculated by the ratio among total valence of the oxidants and fuel (reducing agent), which make it possible to figure out the stoichiometric mixture when the ratio is about 1^{22,23}. The precursors NH₄NO₃ (12.8 g, 160 mmol), (NH₄[NbO(C₂O₄)₂](H₂O)₂) (3.40 g, 10 mmol), [Fe(NO₃)₃·9H₂O] (4.00 g, 10 mmol) and O=C(NH₂)₂ (4.00 g, 66 mmol) were dissolved in 20 mL of distilled water and then transferred to a vitreous silica crucible. The crucible containing the solution was heated in a microwave oven (maximum power 700W) at a frequency of 2.45 GHz. As the solution boils, it dehydrates and the subsequent decomposition produces large amount of gases.

The mixture begins to burn when it reaches the point of spontaneous combustion, releasing heat, liberating vapours and forming the desired phase. After 10 min of reaction, the resulting product was cooled at room temperature, washed with hot water, to remove some residue, and then it was centrifuged and dried at 100 degrees. After these steps, the material was characterized.

2.3 Characterization

The phases of FeNbO₄ were determined by powder X-ray diffraction (PXRD) patterns, collected in a Shimadzu Diffractometer model XRD-7000, with a current of 30 mA and a voltage of 30 kV, using the CuKα radiation (λ = 1.541838 Å). The analysis was conducted in the 2θ range from 10° to 70° with a scanning rate of 1°/min. The obtained patterns were compared to those data deposited at JCPDS (International Centre for Diffraction Data®). The ⁵⁷Fe-Mössbauer experiments were carried out in a spectrometer CMTE model MA250 with a ⁵⁷Co/Rh source at room temperature using α-Fe as reference. The nanometric particle size and the morphology were analyzed using a VEGA3 TESCAN-scanning electron microscope, and transmission electron microscope Tecnai G2-20 - SuperTwin FEI - 200 kV) in the image and electron diffraction mode. For SEM experiments, the samples were dispersed in acetone in an ultrasonic bath, with the aid of a Pasteur pipette. The formed suspension was subsequently dripped on the aluminium support. The size distribution of particle was determined using dynamic light scattering and phase analysis light scattering in a Zetasizer Nano-ZS equipped with 40 mW, 633 nm laser (Model ZEN 360, Malvern Instruments Ltd, Malvern, UK). The specific surface area was determined by the gas adsorption method developed by Brunauer, Emmett and Teller (BET), using a Micromeritics ASAP 2020 surface area and a pore size analyzer. Before measurements, the sample was degassed at 130 °C for up to 48 h under vacuum. The approximate particle size was estimated based on the specific surface area, using Equation 1²⁴:

$$D_{BET} = \frac{6}{D_t \cdot S_{BET}} \quad (1)$$

where: D_{BET} is the equivalent spherical diameter (nm), D_t is the theoretical density (g/cm³) and S_{BET} is the surface area (m²/g).

2.4 Catalytic tests

The catalytic tests were performed in a batch reactor equipped with reaction flask and a magnetic stirrer, operating at 1050 rpm, rotation necessary to keep the solid suspended and dispersed throughout the solution. For the tests, 45 mg of catalyst was used for 50 mL of Indigo Carmine dye solution with a concentration of 50 mg·L⁻¹. Moreover, 500 μL of hydrogen peroxide (H₂O₂, 30% w/v) was added to the system. Adsorption tests were done with an experimental design similar to the catalyst tests, however, in the absence of H₂O₂. Experiments in the absence of the catalyst and the presence of H₂O₂ were also conducted to evaluate the degradation of IC with peroxide. All experiments were carried out in dark to avoid the influence of photolytic processes.

The catalytic experiments were conducted for 6 hours, and every 60 minutes an aliquot of 3 mL was collected, and immediately centrifuged to remove the catalyst and for subsequent analyses. Spectrophotometric measurements were performed on Shimadzu equipment UV-vis model UV 2700, using as a parameter the absorbance value of the maximum absorption wavelength of the dye, which for the IC is 610 nm.

2.5 Decomposition of H₂O₂

The catalytic potential of the H₂O₂ decomposition material was also tested. The system consists of the displacement of the water column in an inverted burette, originating from the formation of gaseous oxygen by the reaction between H₂O₂ and the catalyst. A volume of 7.00 mL of a solution, 30% of H₂O₂ and 45.0 mg of catalyst were used in the experiment.

2.6 Catalyst Reuse

To reuse and recycle the catalytic system, the used Fe-Nb catalyst was collected by centrifugation, washed with water, dried at 100°C and reused in five cycles of degradation.

3. Results and Discussion

The reaction of [Fe(NO₃)₃·9H₂O] with NH₄[NbO(C₂O₄)₂(H₂O)₂] (H₂O) was performed in the presence of NH₄NO₃ and urea. The FeNbO₄ was obtained after 10 minutes of reaction in a microwave oven.

3.1 Diffraction of X-rays (XRD)

The crystalline structure of prepared FeNbO₄ powder was evaluated by XRD analysis. Figure 1 shows the XRD patterns of this material, revealing its crystalline nature, without further treatment. This result indicates that the diffraction peaks were indexed to the FeNbO₄, belonging to the monoclinic symmetry with a space group of P2/c, a typical structure of the wolframite¹⁰, following the ICDD file number 70-2275. This phase indicates that the reaction occurred in a temperature lower than 1085 °C^{10,11,13,15,16}. Moreover, some additional weak reflections were found in the XRD patterns (marked by *), which correlated with the tetragonal structure of Fe₂O₃ (ICDD file no. 89-598)^{10,11}. The XRD results also suggest a small crystallite size of the material, due to the line broadening of the peaks^{25,26}. The average crystallite size was calculated from the full-width at half-maximum (FWHM) of the (111) reflection peak (strongest reflection) by applying Scherrer's equation²⁶. The average crystallite size was around 16 nm.

3.2 Mossbauer spectroscopy

The ⁵⁷Fe Mossbauer Spectroscopic results at room temperature showed the presence of Fe(III) (Figure 2 and

Table 1). Figure 2 displayed a central doublet and a sextet. From the hyperfine parameters (Table 1), the sextet can be associated with the presence of Fe(III) and α-Fe₂O₃ as impurities²⁷. According to Silva et al.²⁸, a magnetic hyperfine field (B_{hf}) distribution with maximum probability value at 50.5 T, as shown in Table 1, is characteristic of hematite. The doublet can be assigned to a Fe (III) with octahedral coordination (δ = 0.39 mm·s⁻¹) as in the wolframite²⁹. This solid is formed by a series of zigzag chains of edge-sharing NbO₆ and FeO₆ octahedral along the [001] direction, with the ordering of Fe(III) and Nb(V), accommodated in the chains²⁹.

3.3 Scanning electron microscopy (SEM)

SEM images of the sample are given in Figure 3. The micrographs show that the prepared material has no preferred morphology. It is also observed that Fe-Nb is composed of micrometric and nanometric agglomerates.

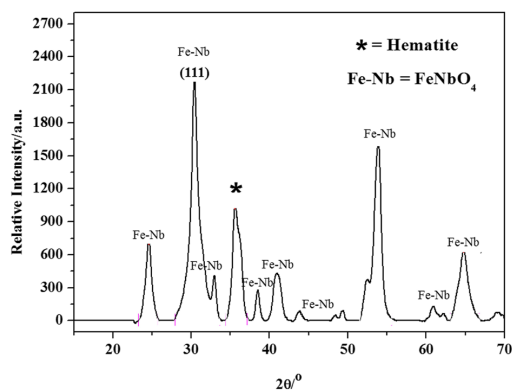


Figure 1. X-ray diffraction pattern of Fe-Nb powder synthesized from combustion reaction.

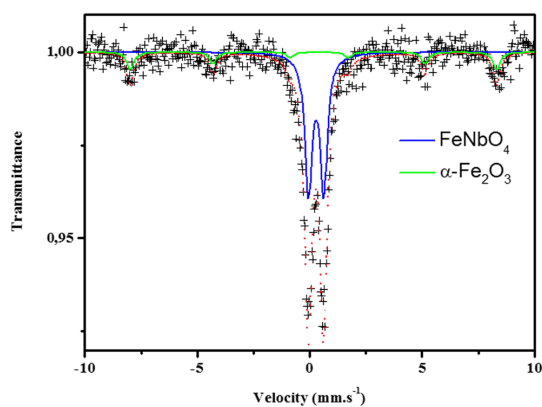


Figure 2. Mössbauer Spectroscopy for the Fe-Nb at room temperature.

Table 1. ⁵⁷Fe Mossbauer parameters for Fe-Nb at room temperature.

Sample	Hyperfine parameters			Iron site	Compound
	δ (mm·s ⁻¹)	Δ ou ε (mm·s ⁻¹)	B _{hf} (T)		
Fe-Nb	0.39	0.58	-	Fe ³⁺	FeNbO ₄
Fe ₂ O ₃	0.39	-0.24	50.51	Fe ³⁺	α-Fe ₂ O ₃

δ = isomer shift relative to αFe. Δ = quadrupole splitting. B_{hf} = magnetic hyperfine field.

The observed agglomeration is a characteristic of materials with nanometric dimensions^{24,25}. Some spherical agglomeration is apparent at high magnification (Figure 3b), with a diameter in the range of 80-180 nm. This result shows the potential of this new approach to produce nanometric structures at high temperatures (around 1085 °C) and at low reaction time¹⁸. The material displays a high crystallinity, a relevant characteristic necessary in catalytic processes since the crystalline phase of some oxides affects catalytic activity³⁰.

3.4 Nitrogen adsorption

The nitrogen adsorption measurements showed a specific surface area (SSA) of 40 m² g⁻¹, characteristic of similar materials obtained by other chemical methods²⁷. Also, using the data obtained by nitrogen adsorption and the BET method, together with Equation 1, it was possible to calculate the average particle size, which is estimated at approximately 42 nm.

3.5 Particle size distribution (DLS)

The dynamic light scattering analysis, confirmed the high degree of agglomeration of the nanoparticles, as revealed by SEM. A particle size distribution near 1000 nm was

obtained. It is worth mentioning that particle agglomeration in nanometric materials is a common phenomenon³¹.

3.6 Transmission electron microscopy (TEM)

High-resolution transmission electron microscopy (HRTEM) was used to better estimate the size of the formed particles. Figure 4, shows the spherical shape and uniform particle size of the material, consisting only of nanoparticle agglomerates, relatively common for nanostructured materials possible induced by high surface energy. It is known that the smaller the particle size the greater the surface tension, which generates a driven force that increases agglomeration. With some of these particles, it was possible to estimate their approximate diameter, their values were between 13 and 20 nm. This leads to the conclusion that the values found, corroborate with the value by calculating Scherrer's equation, for the average crystallite size.

The fast Fourier transform (FFT) was calculated to provide a better view of the inter-planar distances in the material in the HRTEM images. The dots in the graph indicates the periodicity of elements in the MET images, which in this case are the crystalline planes. The dots were isolated from the noise, and the inverse Fourier transform (Inverse FFT)

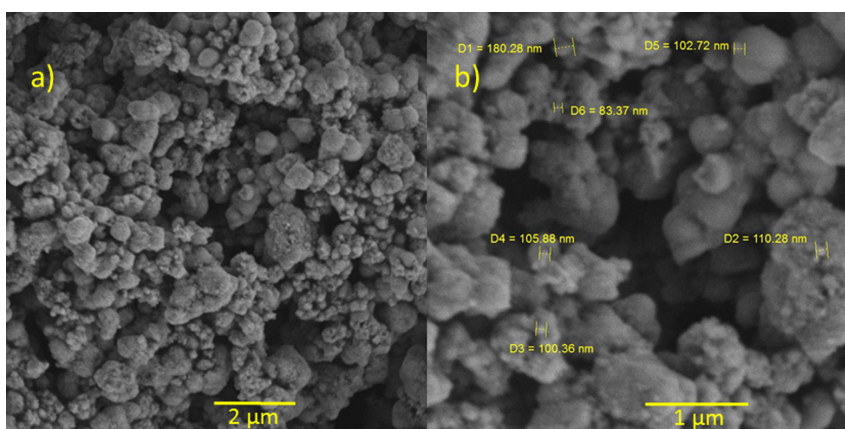


Figure 3. SEM micrographs of the Fe-Nb powder prepared.

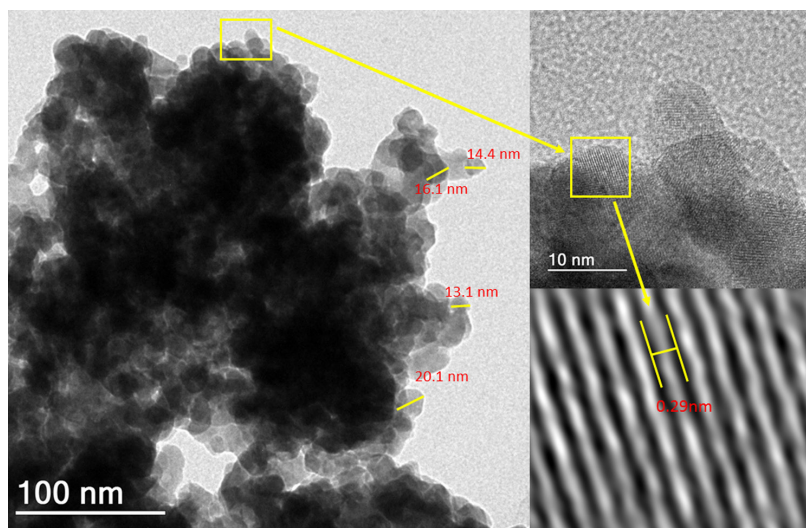


Figure 4. High-resolution transmission electron microscopy (HRTEM) images and the result of the treatment of the Fourier transform for Fe-Nb.

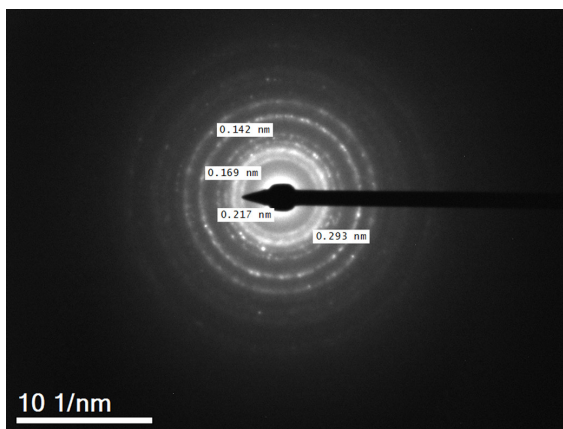


Figure 5. Electron diffraction for Fe-Nb material.

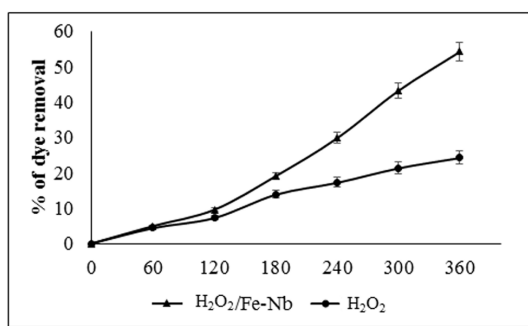


Figure 6. Percent of color removal of IC solutions by the H₂O₂/Fe-Nb and H₂O₂ systems.

was used to recompose the microscopy image. With this process a cleaner image was obtained, which evidences the crystallographic planes, allowing the measurement of inter-planar distances from HRTEM images. This process is shown in Figure 4, on the right side. The distance found (0.29 nm) refers to the 111 planes of the wolframite type structure of FeNbO₄, which corresponds to the most intense peak in the diffractogram (Figure 1).

Figure 5 shows the image obtained by electron diffraction for the material, where it is evident the interplanar distance of the 111 plan family of FeNbO₄, among the other interplanar distances of iron niobate³².

3.7 Catalytic tests

The aim of this tests was to determine the efficiency of the FeNbO₄ in the transformation of H₂O₂ into radicals that in turn would degrade indigo carmine (IC). The experiments were monitored using UV-Vis Spectroscopy measurements in λ_{max} of the dye (610 nm). Before catalytic tests, the Fe-Nb/dye system was left under stirring in the absence of peroxide to investigate the adsorption process. The results revealed insignificant adsorption. According to Subbulekshmi and Subramanian⁹, this is an advantageous catalytic feature because excessive adsorption sometimes hinders the dye degradation or reduce the catalytic efficiency. Figure 6 shows the percentage of removal of the dye IC by the two systems: H₂O₂, and H₂O₂/Fe-Nb.

It is observed in Figure 6, that the H₂O₂/Fe-Nb system is more efficient than H₂O₂ to degrade the IC. A significant increase in the speed of the process is obtained at 150 minutes of reaction as a function of the presence of the catalyst. After 360 min, the H₂O₂/Fe-Nb system causes a reduction of 50% in the concentration of the dye, while a maximum efficiency of 20% was reached by H₂O₂ alone. This higher efficiency is clearly due to the presence of the catalyst in the reaction medium since no other process is acting in parallel to consume IC. It is worth mentioning that FeNbO₄ do not adsorb the dye, therefore the removal of colour from the solution does not relate to a surface phenomenon, but to a chemical oxidation that occurs in the liquid phase, promoted by the systems H₂O₂ and H₂O₂/Fe-Nb. The decomposition of H₂O₂ into radicals, and subsequent decomposition of IC, is little influenced by the hematite, present in the material as a contaminant. Some works reported in the literature show that the presence of Nb(V), sharing the structure in materials with Fe(III) the structure in materials enhances the formation of radicals from hydrogen peroxide, in this cases monitored by the discoloration of methylene blue^{27,28}. In these works, it is clear that the hematite/H₂O₂ system does not generate radicals capable of promoting the degradation of organic molecules in an aqueous medium^{27,28}. Given the above, it is evident that the system responsible for generating radicals, which subsequently degrade the IC is H₂O₂/Fe-Nb. Photolytic events are also disregarded in this case, since the experiments were conducted in the absence of light. It is important to emphasize that it is the first time the literature reports the catalytic oxidation of an organic molecule effected by FeNbO₄ in the presence of H₂O₂.

Finally, it was also possible to investigate the kinetics of the two systems with the degradation data, which fits well with first-order kinetics. Correlation coefficients of 0.97 and 0.99 for the H₂O₂/Fe-Nb and H₂O₂ systems were obtained, respectively. Linear regression provided a constant rate of 2.86 X 10⁻³ min⁻¹ for the H₂O₂/Fe-Nb system with a standard error of 2.31 X 10⁻⁴, and 7.51 X 10⁻⁴ min⁻¹, with an error of 2.72 x 10⁻⁵ for the system containing the peroxide, only. It reveals that the reaction catalyzed by FeNbO₄ has a constant almost 4 times greater than the non-catalyzed one, showing the influence of the catalyst and the efficiency in the degradation of the IC in solution.

3.8 Catalyst reuse

The material had its catalytic potential measured in successive reaction cycles. The results were normalized, therefore the activity equal to 100%, corresponds to the maximum removal efficiency obtained in the first catalysis experiment, that is, where the catalyst degrades about 50% of the dye solution. Figure 7 shows that the material maintained more than 60% of its efficiency even after four catalytic cycles, which corresponds to a degradation of approximately 30% of the IC solution, still superior to the degradation promoted by peroxide alone.

According to Klimov et al.³³ and Budroni et al.³⁴, the loss of activity can occur by several different factors^{33,34}. Among them the loss of catalyst during the process of separation and the deactivation of active sites as a function of the adsorption of some species present in solution.

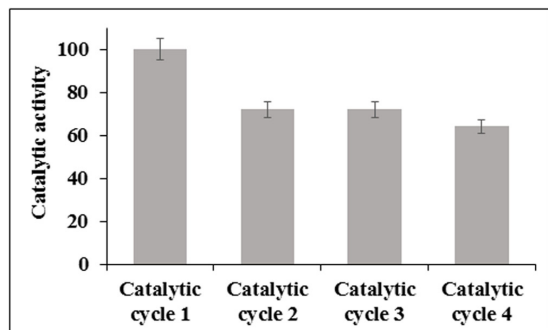


Figure 7. Activity of the catalyst X catalytic cycles.

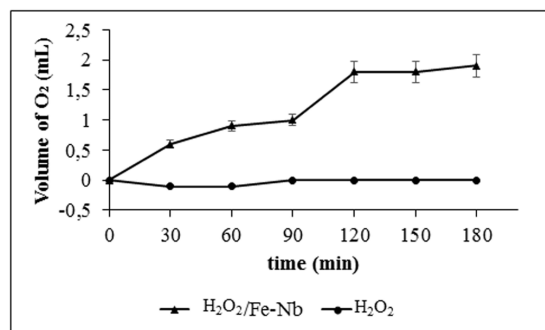


Figure 8. Evolution of the volume of O₂ as a function of the decomposition of H₂O₂.

Considering the characteristics of this reaction, both loss of material and deactivation of sites may have happened. The nanoscale nature of the material prevents efficient decantation even by when the solution is centrifuged. On the other hand, it is likely possible the adsorption of chemical species on the surface of the catalyst.

3.9 Decomposition reactions of H₂O₂

The H₂O₂ decomposition experiments demonstrated indirectly the potential of a material to generate hydroxyl radicals in solution³⁵. The decomposition of the peroxide is measured by the displacement of water inside the burette, which occurs as a function of the O₂ generated in the reaction.

The results show (Figure 8) that the presence of the material accelerates the H₂O₂ disproportionation, making it an essential material for a successful catalytic process based on radical HO· or HOO·.

As mentioned before other Nb(V)-containing materials and iron oxides have already been investigated in advanced oxidation processes in the presence of hydrogen peroxide^{26,35,36}. In these works, the authors promote the oxidation of organic molecules with doped oxides or a mixture of oxides of these two metals {Nb(V) and Fe(III)}, synthesized mainly by the co-precipitation method. In the present work, we are showing the unprecedented synthesis of the FeNbO₄ by microwave-assisted combustion reaction. Additionally, it shows the potential of the obtained material to generate radicals in solution in the presence of H₂O₂ and to promote the oxidation of organic contaminants.

Although the mechanism is still unclear, it is possible to say that it is not by the interaction of the molecule with the surface of the material, since the adsorption is insignificant. Therefore, the discoloration of the solution is probably promoted by radical species formed in the interaction between the peroxide and the material. According to the literature, peroxy-metal and hydroperoxy-systems are important classes of oxidants³⁶. Peroxy-metal complexes are formed rapidly in water over a wide pH range from a variety of metal compounds, mainly of groups IV, V and VI, notably titanium (IV), vanadium (V), molybdenum (VI) and tungsten (VI)³⁷. Although these systems are promising, they are still little explored in wastewater decontamination.

4. Conclusions

FeNbO₄ nanoparticles with wolframite structure were synthesized by microwave-assisted combustion reaction for the first time and their catalytic properties were investigated. This novel combustion method provides a rapid and reproducible route for the preparation of crystalline iron niobate powders. The route was efficient to obtain FeNbO₄ in a single crystalline system since this material has polymorphism^{15,16}. A secondary phase of hematite was observed, which according to the literature is common due to the complex phase diagram of the Fe₂O₃-Nb₂O₅ system. In this phase diagram, the isomorphous replacement of Nb(V) by Fe(III) tends to cause significant structural changes for the formation of iron(III) niobate, with three modifications in the formal composition of this compound being known. Also, in some cases, part of the precursor Fe₂O₃ used in the synthesis process may remain in the system as a second phase due to the need of long thermal treatments to obtain the FeNbO₄^{10,15,16}. Although this phase occurred, it was not an impediment to assess the catalytic properties of iron niobate. The crystallite size was estimated at ~13 to 20 nm. This one-pot procedure offered a quicker reaction time to prepare iron(III) niobate, as well as a shorter heating time, provided by the microwave (approximately 10 min), preventing, this way, excessive particle growth. The results demonstrated that Fe-Nb has good catalytic activity, removing twice more dye in solution than the non-catalyzed reaction. Applicability of the developed heterogeneous catalyst for repeated use was also confirmed by the sustainability of the efficiency of the catalyst, even on 4th catalytic run. Reactions of H₂O₂ decomposition in the presence of the catalyst and also in its absence indirectly shown that the material is capable of generating more radicals in solution than the non-catalyzed reaction. Finally, the present work shows that H₂O₂/FeNbO₄ system may be a potential technology for the removal of organic contaminants in aqueous solution.

5. Acknowledgements

Authors would like to thank CNPQ and FAPEMIG for financial support.

6. References

1. Husain Q. Peroxidase mediated decolorization and remediation of wastewater containing industrial dyes: a review. *Rev Environ*

- Sci Biotechnol. 2010;9:117-40. <http://dx.doi.org/10.1007/s11157-009-9184-9>.
2. Singh K, Arora S. Remove of synthetic textile dyes from wastewaters: a critical review on present treatment. *Technologies (Basel)*. 2011;41(9):807-78. <http://dx.doi.org/10.1080/10643380903218376>.
 3. Othman I, Mohamed RM, Ibrahim FM. Study of photocatalytic oxidation of indigo carmine dye of Mn-supported TiO₂. *J Photochem Photobiol Chem*. 2007;189:80-5. <http://dx.doi.org/10.1016/j.jphotochem.2007.01.010>.
 4. Andrade FV, Lima GM, August R, Coelho MG, Pertence Y, Machado IR, et al. Use of hydroxyapatite Ca₅(PO₄)₃OH obtained from refuse of cattle slaughterer as a catalyst support: an alternative material for heterogeneous photocatalysis. *J Sci Res Stud*. 2017;4(10):245-253.
 5. Andrade FV, Lima GM, August R, Silva JCC, Paniago R, Coelho MG, et al. A novel TiO₂/autoclaved cellular concrete composite: from a precast building material to a new floating photocatalyst for degradation of organic water contaminants. *J Water Process Eng*. 2015;7:27-35. <http://dx.doi.org/10.1016/j.jwpe.2015.04.005>.
 6. Andrade FV, Lima GM, August R, Coelho MG, Pertence Y, Machado IR. A new material consisting of TiO₂ supported on Nb₂O₅ as photocatalyst for the degradation of organic contaminants in aqueous medium. *J Environ Chem Eng*. 2014;2:2352-8. <http://dx.doi.org/10.1016/j.jece.2014.02.004>.
 7. Andrade FV, Lima GM, August R, Coelho MG, Ardisson JD, Romero OB. A versatile approach to treat aqueous residues of textile industry: the photocatalytic degradation of Indigo Carmine dye employing the autoclaved cellular concrete/Fe₂O₃ system. *Chem Eng J*. 2012;180:25-31. <http://dx.doi.org/10.1016/j.cej.2011.10.089>.
 8. Singh L, Reka P, Chand S. Cu-impregnated zeolite Y as highly active and stable heterogeneous Fenton-like catalyst for degradation of Congo Red dye. *Separ Purif Tech*. 2016;170:321-36. <http://dx.doi.org/10.1016/j.seppur.2016.06.059>.
 9. Subbulekshmi NL, Subramanian E. High degree Fenton-like catalytic activity of CuO/zeolite X catalyst from coal fly ash in mineralization of Indigo Carmine dye. *J. Environment and Biotechnology Research*. 2017;6(2):228-37.
 10. Ananta S, Brydson R, Thomas NW. Synthesis, formation and characterisation of FeNbO₄ powders. *J Eur Ceram Soc*. 1999;19:489-96. [http://dx.doi.org/10.1016/S0955-2219\(98\)00219-2](http://dx.doi.org/10.1016/S0955-2219(98)00219-2).
 11. Devesa S, Graça MP, Henry F, Costa LC. Dielectric properties of FeNbO₄ ceramics prepared by the sol-gel method. *Solid State Sci*. 2016;61:44-50. <https://doi.org/10.1016/j.solidstatesciences.2016.09.005>.
 12. Shim H-W, Cho I-S, Hong KS, Lim A-H, Kim D-W. Hydrothermal synthesis and electrochemical properties of FeNbO₄ nanospheres. *J Ceram Soc Jpn*. 2012;120(2):82-5. <http://dx.doi.org/10.2109/jcersj2.120.82>.
 13. Cho I-S, Lee S, Noh JH, Choi GK, Jung HS, Kim DW, et al. Visible light-induced photocatalytic activity in FeNbO₄ nanoparticles. *J Phys Chem C*. 2008;112:18393-8. <http://dx.doi.org/10.1021/jp807006g>.
 14. Li QJ, Xia SQ, Wang XY, Xia W, Yu Y, Cui YM, et al. The colossal dielectric properties of FeNbO₄. *J Alloys Compd*. 2014;616:577-80. <http://dx.doi.org/10.1016/j.jallcom.2014.07.104>.
 15. Ehrenberg H, Wltschek G, Theissmann R, Weitzel H, Fuess H, Trouw F. The magnetic structure of FeNbO₄. *J. Magnetism and Magnetic Materials*. 218;2000:261-65. [http://dx.doi.org/10.1016/S0304-8853\(00\)00395-4](http://dx.doi.org/10.1016/S0304-8853(00)00395-4).
 16. Theissmann R, Ehrenberg H, Weitzel H, Fuess H. Domain structure and lattice strains in FeNbO₄. *Solid State Sci*. 2005;7:791-5. <http://dx.doi.org/10.1016/j.solidstatesciences.2004.11.027>.
 17. Freitas MR, Gouveia GL, Costa LJD, Oliveira AJA, Kiminami RHGA. Microwave assisted combustion synthesis and characterization of nanocrystalline nickel-doped cobalt ferrites. *Mater Res*. 2016;19(Suppl. 1):27-32. <http://dx.doi.org/10.1590/1980-5373-MR-2016-0077>.
 18. Jain SR, Adiga KC, Pai Verneker VR. A new approach to thermochemical calculations of condensed fuel-oxidizer mixtures. *Combust Flame*. 1981;40:71-9. [http://dx.doi.org/10.1016/0010-2180\(81\)90111-5](http://dx.doi.org/10.1016/0010-2180(81)90111-5).
 19. Freitas NL, Coutinho JP, Silva MC, Lira HL, Kiminami RHGA, Costa ACFM. Synthesis of Ni-Zn ferrite catalysts by Combustion reaction using different fuels. *Mater Sci Forum*. 2010;660-661:943-7. <http://dx.doi.org/10.4028/www.scientific.net/MSF.660-661.943>.
 20. Nehru LC, Sanjeeviraja C. Microwave-assisted combustion synthesis of nanocrystalline ZnO powders using zinc nitrate and various amount of organic fuels as reactants: influence of reactant parameters – A status review. *Nano Hibrids*. 2014;6:75-110. <http://dx.doi.org/10.4028/www.scientific.net/NH.6.75>.
 21. Costa AC, Kiminami RH, Morelli MR. Combustion synthesis processing of nanoceramics. *Handbook of nanoceramics their based nanodevices*. California: American Scientific Publishers; 2009. p. 375-392.
 22. Kiminami RHGA, Morelli MR, Folz DC, Clark DE. Microwave synthesis of alumina powders. *Am Ceram Soc Bull*. 2000;79:63-7.
 23. Nakagomi F, Cerruti SE, Roberto de Freitas M, Freitas ES No, Andrade FV, Siqueira GO. Niobium pentoxide produced by a novel method microwave assisted combustion synthesis. *Chem Phys Lett*. 2019;729:37-41. <http://dx.doi.org/10.1016/j.cplett.2019.05.003>.
 24. Singhal S, Singh J, Barthwal SK, Chandra K. Preparation and characterization of nanosize nickel-substituted cobalt ferrites (Co_{1-x}Ni_xFe₂O₄). *J Solid State Chem*. 2005;178(10):3183-9. <http://dx.doi.org/10.1016/j.jssc.2005.07.020>.
 25. Mangalaraja RV, Mouzon J, Hedström P, Camurri CC, Ananthakumar S, Odén M. Microwave assisted combustion synthesis of nanocrystalline yttria and its powder characteristics. *Powder Technol*. 2009;191(3):309-14. <http://dx.doi.org/10.1016/j.powtec.2008.10.019>.
 26. Cullity BD. *Elements of X-ray diffraction*. Reading: AddisonWesley; 1987.
 27. Silva AC, Cepera RM, Pereira MC, Lima DQ, Fabris JD, Oliveira LCA. Heterogeneous catalyst based on peroxoniobium complexes immobilized over iron oxide for organic oxidation in water. *Appl Catal B*. 2011;107:237-44. <http://dx.doi.org/10.1016/j.apcatb.2011.07.017>.
 28. Silva AC, Oliveira DQL, Oliveira LCA, Anastácio AS, Ramalho TC, Lopes JH, et al. Nb-containing hematites Fe_{2-x}Nb_xO₃: the role of Nb⁵⁺ on the reactivity in presence of the H₂O₂ or ultraviolet light. *Appl Catal A Gen*. 2009;357:79-84. <http://dx.doi.org/10.1016/j.apcata.2009.01.014>.
 29. Schmidbauer E, Schneider J. Electrical resistivity, thermopower, and ⁵⁷Fe mossbauer study of FeNbO₄. *J Solid State Chem*. 1997;134:253-64.
 30. Paunović V, Pineiro MR, Lopez N, Ramirez JP. Activity differences of rutile and anatase TiO₂ polymorphs in catalytic HBr Oxidation. *Catal Today*. 2020. <http://dx.doi.org/10.1016/j.cattod.2020.03.036>.
 31. Tsuda A, Venkata NK. The role of natural processes and surface energy of inhaled engineered nanoparticles on aggregation and corona formation. *NanoImpact*. 2016;2(2):38-44. <http://dx.doi.org/10.1016/j.impact.2016.06.002>.
 32. Cho IS, Lee S, Noh JH, Choi GK, Jung HS, Kim DW, et al. Visible-light-induced photocatalytic activity in FeNbO₄ nanoparticles. *J Phys Chem C*. 2008;112:18393-8. <http://dx.doi.org/10.1021/jp807006g>.
 33. Klimov MEM, Hipólito PH, Garcia MM, Klimova TE. Pd catalysts supported on hydrogen titanate nanotubes for Suzuki-Miyaura cross coupling reactions. *Calalysis Today*, 2018;305:58-64. <http://dx.doi.org/10.1016/j.cattod.2017.10.015>.
 34. Budroni G, Corma A, Garcia H, Primo A. Pd nanoparticles embedded in sponge like porous silica as a Suzuki-Miyaura

- catalyst: similarities and differences with homogeneous catalysts. *J Catal.* 2007;251(2):345-53. <http://dx.doi.org/10.1016/j.jcat.2007.07.027>.
35. Oliveira LCA, Ramalho TC, Souza EF, Gonçalves M, Oliveira DQL, Pereira MC, et al. Catalytic properties of goethite prepared in the presence of Nb on oxidation reactions in water: computational and experimental studies. *Appl Catal B.* 2008;83:169-76.
 36. Oliveira LCA, Gonçalves M, Guerreiro MC, Ramalho TC, Fabris JD, Pereira MC, et al. A new catalyst material based on niobia/iron oxide composite on the oxidation of organic contaminants in water via heterogeneous Fenton mechanisms. *Appl Catal A Gen.* 2007;316:117-24. <http://dx.doi.org/10.1016/j.apcata.2006.09.027>.
 37. Jones CW, Clark JH. Activation of hydrogen peroxide using inorganic and organic species. USA: Royal Society of Chemistry; 2007. <http://dx.doi.org/10.1039/9781847550132-00037>.